INTERNATIONAL JOURNAL FOR NUMERICAL AND ANALYTICAL METHODS IN GEOMECHANICS, VOL. 20, 35–56 (1996)

ANALYTICAL MODEL OF PROGRESSIVE SLOPE FAILURE IN WASTE CONTAINMENT SYSTEMS

ROBERT B. GILBERT*

Cockrell Hall, The University of Texas, Austin, TX 78712, U.S.A.

JAMES H. LONG†

MC-250, University of Illinois, 205 N. Mathews Ave., Urbana, IL, U.S.A.

AND

BARRY E. MOSES‡

Cockrell Hall, The University of Texas, Austin, TX 78712, U.S.A.

SUMMARY

The potential for progressive failure in waste containment systems is an important design consideration. Many common interfaces between components in containment systems exhibit strain-softening behaviour; however, slopes are presently designed using limit equilibrium methods that do not account for these effects. An analytical model is developed to investigate the potential for progressive failure due to strain softening. Results are presented in a non-dimensional form relating the potential for strain softening to the slope geometry, the waste properties and the properties of the containment system interface. The potential for progressive failure increases as (i) the waste stiffness decreases relative to the initial stiffness of the interface resistance, (ii) the length of the slip surface increases and (iii) the rate of strain softening with displacement increases. Analysis of a case study slope failure indicates that the analytical approach produces results that are consistent with field observations and comparable to results from a more sophisticated, numerical analysis. Although simple, this analytical approach serves as a useful design guide to identify cases where it is unsafe to use the peak shear strength in a limit equilibrium analysis.

KEY WORDS: waste containment systems; slope failure; strain-softening; landfill

INTRODUCTION

Modern waste containment facilities, such as landfills, waste piles and impoundments, are equipped with sophisticated lining and cover systems to contain waste and protect the environment. Components in these containment systems include soil materials (e.g. compacted clay liners and granular drainage layers) and geosynthetic materials (e.g. geomembranes, geotextiles and geonets). Slope stability is an important consideration in the design of containment systems (Figure 1). Recent laboratory shear testing results indicate that many common interfaces between components in waste containment systems exhibit strain-softening behaviour (e.g. Reference 1). A peak shear strength is developed at a small relative displacement, typically less than 15 mm. With additional continuous displacement, the shear strength decreases and ultimately

* Assistant Professor of Civil Engineering
† Associate Professor of Civil Engineering
‡ Graduate Research Assistant

CCC 0363–9061/96/010035–22
© 1996 by John Wiley & Sons, Ltd.
Received 18 June 1994
Revised 13 June 1995

approaches a residual value. For example, a direct shear test result is shown in Figure 2 for the interface between a geomembrane and a compacted clay liner.

Slopes in waste containment systems are commonly designed using a limit equilibrium approach: the available or limiting shear resistance along a potential slip surface is compared with the shear resistance required to maintain equilibrium. It is difficult to establish the available shear resistance along an interface exhibiting strain-softening behaviour, and it may be unsafe to assume that the peak strength is available along the entire slip surface. Analyses of a major slope failure in a waste containment system indicate that strain-softening behaviour contributed to the failure.[1,2] However, it may be excessively conservative and costly to assume that only the residual strength is available. The available shear resistance will lie between these two extremes, and it will be related to the level of deformation in the system.

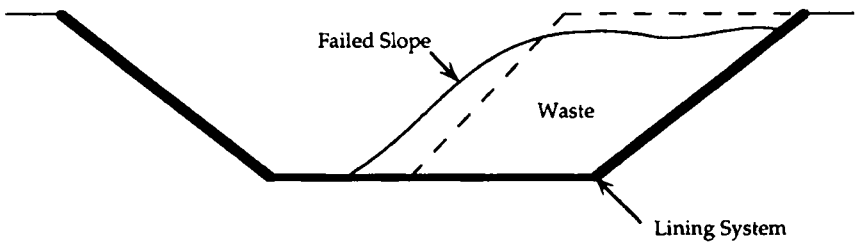

Figure 1. Slope failure in a containment system

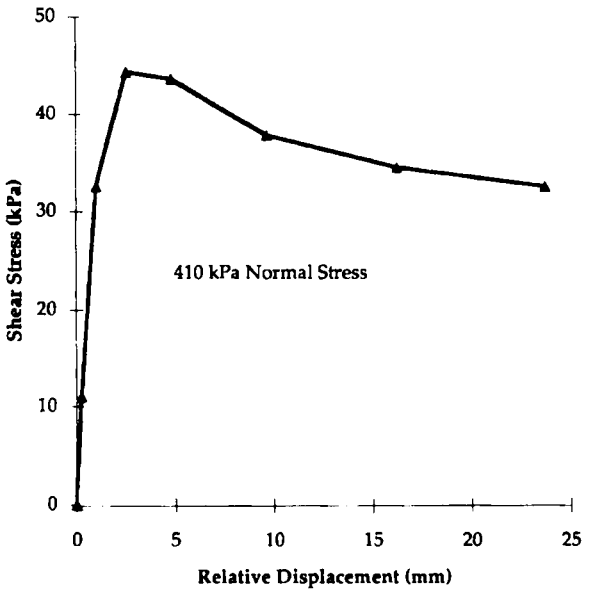

Figure 2. Shear stress versus displacement results for an interface between a geomembrane and a compacted clay liner (data from Byrne *et al.*[1])

Numerous researchers have investigated the effect of strain softening on the stability of soil slopes using numerical models to maintain compatibility between stresses and strains. These analyses addressed both one-dimensional[3,4] and two-dimensional[5-7] conditions. In addition, Byrne[8] used a finite difference technique to explore how strain-softening behaviour affects the stability of slopes in waste containment systems. He drew the following conclusions: (1) limit equilibrium analyses can provide misleading and non-conservative assessments of stability; (2) limit equilibrium results become less applicable as the rate of strain softening with displacement increases and (3) numerical methods that maintain compatibility between stresses and strains should be used to perform stability analyses. Although numerical techniques such as finite element and difference methods have been available for more than 30 years, they have found limited use in geotechnical practice for slope design. Further, the level of effort required to model individual cases limits our ability to perform extensive sensitivity studies and to draw general conclusions.

In this paper, we present an analytical model for evaluating strain-softening effects on the stability of waste containment systems. Although simple, this model provides an effective tool for assessing the potential of progressive failure due to strain softening. Similar approaches have been proposed by Christian and Whitman[9] to model progressive failure of excavated slopes in strain-softening soils and by Murff[10] and Randolph[11] to evaluate axial capacity of piles in strain-softening soils. This paper extends these works to model strain-softening behaviour in waste containment slopes. Results are summarized in a non-dimensional form that relates strain-softening behaviour to the slope geometry, the interface properties and the waste properties. These non-dimensional results serve as a useful design guide to help identify cases where it is unsafe to use the peak shear strength in a limit equilibrium analysis. They also provide convenient means for quantifying the effect of strain-softening behaviour on slope stability.

PROBLEM FORMULATION

A cross-section through a typical containment system slope is shown in Figure 3. This condition represents a below grade landfill cell during filling or a closed landfill in a valley. The waste on the slope is supported by a buttress of waste at the toe. The waste will compress to transmit the driving load in the slope to the buttress, and slippage will occur along the interface to mobilize shear resistance. These deformations may progressively reduce the available shear resistance along the interface due to strain-softening behaviour. In order to model this behaviour, the waste in the buttress and that on the slope are represented by one-dimensional, compressible columns (Figure 3). These columns are linked by a spring at the toe of the slope. The validity of simplifying this two-dimensional cross-section into two one-dimensional columns will be investigated later in this paper.

An idealized representation of strain-softening behaviour at the interface is shown in Figure 4. The peak shear resistance τ_p is mobilized at relative displacement δ_p. As the displacement increases further, the shear resistance decreases until a residual value τ_r is mobilized at relative displacement δ_r. The magnitude of reduction in shear strength due to strain softening is measured by a non-dimensional parameter ζ as follows:

$$\zeta = \frac{\tau_r}{\tau_p} \tag{1}$$

Common interfaces in containment systems have ζ values ranging from 0·3 to 0·8. The rate of post-peak strength reduction with displacement is measured relative to the initial rate of strength

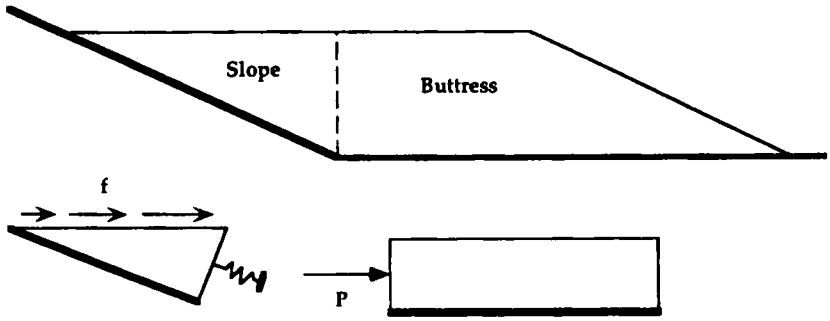

Figure 3. One-dimensional models of compressible waste buttress and slope on strain-softening interfaces

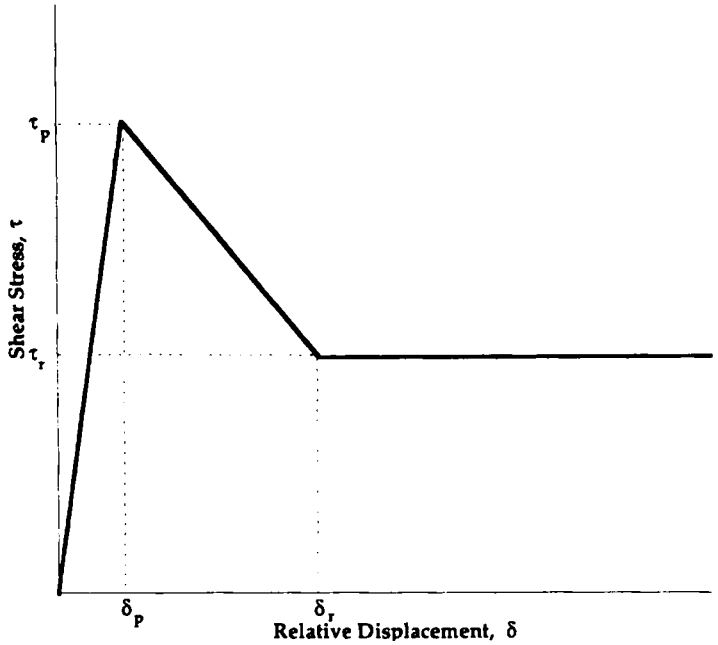

Figure 4. Idealized shear stress versus displacement model for lining system interface

increase using a non-dimensional parameter Ω as follows:

$$\Omega = \frac{-(\tau_r - \tau_p)/(\delta_r - \delta_p)}{\tau_p/\delta_p} \tag{2}$$

As Ω increases, the rate of strain softening with displacement increases. Values for Ω range from 0·0005 to 0·5 for typical interfaces in containment systems.

The maximum available shear resistance along the containment system is found by first evaluating the capacity and stiffness of the buttress. The mobilized shear resistance on the slope is then obtained as a function of the buttress stiffness.

Buttress case

The waste buttress is modelled as a one-dimensional, compressible column on a strain-softening interface (Figure 3). We will assume that the waste behaves as an elastic material in axial compression. This assumption should be reasonable providing that the waste is not near failure, i.e. the critical failure surface is located along the containment system.

General solution. The relative displacement, u, at any point along the interface is obtained from the following partial differential equation describing force equilibrium:

$$\frac{d^2u}{dx^2} = \frac{\tau(u)W_1}{EA_B} \tag{3}$$

where x is the horizontal distance from the left boundary, $\tau(u)$ is the interface shear resistance, E is Young's modulus for the waste, W_1 is the unit width of the buttress and A_B is the cross-sectional area of the buttress ($H_B W_1$ where H_B is the column height). This model assumes that the lateral strains in the buttress above the interface are uniform with depth. Field measurements of strains in soil slopes above well-defined slip surfaces support this assumption.[12] Non-dimensional forms of equation (3) for the possible range of displacements are given as follows:

$$\frac{d^2\upsilon}{d\xi^2} = M\upsilon, \quad \upsilon \leqslant \Delta_p \tag{4a}$$

$$\frac{d^2\upsilon}{d\xi^2} = -M\Omega\upsilon + M(1+\Omega)\Delta_p, \quad \Delta_p < \upsilon \leqslant \Delta_r \tag{4b}$$

$$\frac{d^2\upsilon}{d\xi^2} = \zeta M\Delta_p, \quad \upsilon > \Delta_r \tag{4c}$$

where $\upsilon = u/W_1$, $\Delta_p = \delta_p/W_1$, $\Delta_r = \delta_r/W_1$, $\xi = x/L_B$ and

$$M = \frac{(\tau_p L_B)/\delta_p}{(EH_B)/L_B} \tag{5}$$

where L_B is the buttress length. The general solution for equation (4) is given by

$$\upsilon = a_1 e^{\sqrt{M}\xi} + a_2 e^{-\sqrt{M}\xi}, \quad \upsilon \leqslant \Delta_p \tag{6a}$$

$$\upsilon = b_1 \cos(\sqrt{M\Omega}\xi) + b_2 \sin(\sqrt{M\Omega}\xi) + \left(\frac{1+\Omega}{\Omega}\right)\Delta_p, \quad \Delta_p < \upsilon \leqslant \Delta_r \tag{6b}$$

$$\upsilon = \left(\frac{\xi M\Delta_p}{2}\right)\xi^2 + c_1\xi + c_2, \quad \upsilon > \Delta_r \tag{6c}$$

where a_1, a_2, b_2, c_1 and c_2 are constants that depend on the boundary conditions.

Boundary conditions. The boundary conditions for the column are an external force P applied to the left boundary and no external force applied to the right boundary. In non-dimensional form,

these boundary conditions are given by

$$\left.\frac{d\upsilon}{d\xi}\right|_{\xi=0} = \Phi \tag{7a}$$

$$\left.\frac{d\upsilon}{d\xi}\right|_{\xi=1} = 0 \tag{7b}$$

where

$$\Phi = \left(\frac{P/W_1}{EA_B}\right)L_B \tag{8}$$

On the basis of force equilibrium, the mobilized shear resistance along the interface is equal to $-P$ (a negative force is compressive), or non-dimensionally represented by $-\Phi$. The mobilized shear resistance will be related to the normalized displacement at the left boundary, υ_1. Initially, $-\Phi$ will increase with increasing υ_1. Once υ_1 exceeds Δ_p, the available shear resistance near the left boundary will begin decreasing due to strain softening and the rate of increase in $-\Phi$ with υ_1 will decrease. As υ_1 continues to increase, $-\Phi$ will eventually reach a maximum value and then decrease or remain constant. Ultimately, the residual strength will be mobilized along the entire interface. The maximum available shear resistance is obtained by maximizing $-\Phi$ with respect to υ_1.

In general, the interface will be divided into three zones from left to right: a plastic zone where $\upsilon > \Delta_r$, a transition zone where $\Delta_p < \upsilon \leqslant \Delta_r$, and an elastic zone where $\upsilon \leqslant \Delta_p$. Denoting the proportions of total length in the plastic and transition zones ξ_L and ξ_T, respectively, the solution for υ is obtained from equation (6) by setting $\upsilon = \Delta_r$ at $\xi = \xi_L$ and $\upsilon = \Delta_p$ at $\xi = \xi_L + \xi_T$:

$$\frac{\upsilon}{\Delta_p} = \frac{\zeta M}{2}(\xi^2 - \xi_L^2) + \frac{\Phi}{\Delta_p}(\xi - \xi_L) + \frac{1 - \zeta + \Omega}{\Omega}, \quad 0 \leqslant \xi < \xi_L \tag{9a}$$

$$\frac{\upsilon}{\Delta_p} = \left(\frac{-\zeta}{\Omega}\right)\cos[\sqrt{M\Omega}(\xi - \xi_L)] + \left[\frac{\zeta\cos(\sqrt{M\Omega}\xi_T) - 1}{\Omega\sin(\sqrt{M\Omega}\xi_T)}\right]\sin[\sqrt{M\Omega}(\xi - \xi_L)] + \frac{1 + \Omega}{\Omega}, \quad \xi_L \leqslant \xi < \xi_L + \xi_T \tag{9b}$$

$$\frac{\upsilon}{\Delta_p} = \frac{e^{\sqrt{M}(1-\xi)} + e^{-\sqrt{M}(1-\xi)}}{e^{\sqrt{M}(1-\xi_L-\xi_T)} + e^{-\sqrt{M}(1-\xi_L-\xi_T)}}, \quad \xi_L + \xi_T \leqslant \xi \leqslant 1 \tag{9c}$$

For a given value of Φ, ξ_L and ξ_T are evaluated by maintaining internal equilibrium at the boundary between the plastic and transition zones

$$(\zeta M)\xi_L + \frac{\Phi}{\Delta_p} = \sqrt{\frac{M}{\Omega}}\left[\frac{\zeta\cos(\sqrt{M\Omega}\xi_T) - 1}{\sin(\sqrt{M\Omega}\xi_T)}\right] \tag{10a}$$

and the boundary between the transition and elastic zones

$$\frac{e^{-2\sqrt{M}(1-\xi_L-\xi_T)} - 1}{e^{-2\sqrt{M}(1-\xi_L-\xi_T)} + 1} = \frac{1}{\sqrt{\Omega}}\left[\frac{\zeta - \cos(\sqrt{M\Omega}\xi_T)}{\sin(\sqrt{M\Omega}\xi_T)}\right] \tag{10b}$$

Since ξ_L and ξ_T cannot be solved for explicitly, they are evaluated using a numerical approach. Finally, v_1 is obtained as follows:

$$\frac{v_1}{\Delta_p} = \frac{v|_{\xi=0}}{\Delta_p} = -\frac{\xi M}{2}\xi_L^2 - \frac{\Phi}{\Delta_p}\xi_L + \frac{1-\zeta+\Omega}{\Omega} \tag{11}$$

Both v_1 and Φ are functions of ξ_L; hence, the maximum value of $-\Phi$, $(-\Phi)_{max}$, can be found by maximizing $-\Phi$ with respect to ξ_L in equation (10).

If the peak shear strength is available along the entire interface, then the peak value of Φ is equal to

$$\Phi_{peak} = \frac{-\tau_p L_B^2}{EA_B} \tag{12}$$

and the reduction in mobilized shear resistance is measured by

$$\rho = \frac{\Phi}{\Phi_{peak}} = \frac{-1}{M}\left(\frac{\Phi}{\Delta_p}\right) \tag{13}$$

Maximizing $-\Phi$ is accomplished by maximizing ρ. Rearranging equation (13), we can replace Φ/Δ_p in equation (10) as follows:

$$\rho = \frac{-1}{\sqrt{M\Omega}}\left[\frac{\zeta\cos(\sqrt{M\Omega}\xi_T) - 1}{\sin(\sqrt{M\Omega}\xi_T)}\right] + \zeta\xi_L \tag{14a}$$

$$\frac{e^{-2\sqrt{M}(1-\xi_L-\xi_T)} - 1}{e^{-2\sqrt{M}(1-\xi_L-\xi_T)} + 1} = \frac{1}{\sqrt{\Omega}}\left[\frac{\zeta - \cos(\sqrt{M\Omega}\xi_T)}{\sin(\sqrt{M\Omega}\xi_T)}\right] \tag{14b}$$

The maximum value of ρ, denoted R_f, represents the average reduction in available shear resistance due to strain softening. This reduction factor can range from 1 (no reduction in resistance) to ζ (maximum reduction), and the average available shear resistance along the interface is simply R_f multiplied by τ_p. R_f is found by maximizing ρ in equation (14a) with respect to ξ_L, where ξ_T is related to ξ_L by equation (14b); therefore, R_f is a function only of the fundamental non-dimensional parameters M, ζ and Ω.

The amount of deformation required to mobilize the maximum available shear resistance in the buttress is also of interest. The stiffness that the buttress provides to the adjacent slope (Figure 3) is expressed by

$$Q_{max} = \left[\frac{\Phi_{max}}{(v_1)_{max}}\right]\frac{EA_B}{L_B} \tag{15}$$

where $(v_1)_{max}$ is the displacement at the left boundary corresponding to Φ_{max}. Likewise, if the peak strength is fully mobilized, then the peak value of Q is given by

$$Q_{peak} = \left[\frac{\Phi_{peak}}{\Delta_p}\right]\frac{EA_B}{L_B} \tag{16}$$

The reduction in buttress stiffness due to strain softening can therefore be measured by

$$\mu = \frac{Q_{max}}{Q_{peak}} = \frac{\Phi_{max}/\Phi_{peak}}{(v_1)_{max}/\Delta_p} = \frac{R_f}{(v_1)_{max}/\Delta_p} \tag{17}$$

Substituting equation (11) into equation (17), we obtain the following for μ:

$$\mu = \frac{R_f}{-(\zeta M/2)\xi_L^2 + MR_f\xi_L + (1 - \zeta + \Omega)/\Omega} \tag{18}$$

Hence, the reduction in stiffness due to strain softening is also a function of M, ζ and Ω.

The maximum value of R_f may occur before the plastic zone appears at the left boundary ($\xi_L = 0$) or after the elastic zone disappears from the right boundary ($\xi_L + \xi_T = 1$). In these cases, the solution for υ is developed from equation (6) by modifying the boundary conditions between zones accordingly. For the case $\xi_L = 0$ and $\xi_T < 1$, R_f and μ are found from

$$\rho = \frac{-1}{\sqrt{M}}\left[\cos(\sqrt{M\Omega}\xi_T)\left(\frac{e^{-2\sqrt{M}(1-\xi_T)} - 1}{e^{-2\sqrt{M}(1-\xi_T)} + 1}\right) - \frac{1}{\sqrt{\Omega}}\sin(\sqrt{M\Omega}\xi_T)\right] \tag{19a}$$

$$\mu = \frac{R_f}{\dfrac{-1 + R_f\sqrt{M\Omega}\sin(\sqrt{M\Omega}\xi_T)}{\Omega\cos(\sqrt{M\Omega}\xi_T)} + \dfrac{1+\Omega}{\Omega}} \tag{19b}$$

where R_f is the maximum value of ρ with respect to ξ_T. When $\xi_L = 0$ and $\xi_T = 1$, R_f and μ are obtained from

$$R_f = \frac{1}{\sqrt{M\Omega}}\sin(\sqrt{M\Omega}) \tag{20a}$$

$$\mu = \frac{R_f}{\dfrac{-1 + R_f\sqrt{M\Omega}\sin(\sqrt{M\Omega})}{\Omega\cos(\sqrt{M\Omega})} + \dfrac{1+\Omega}{\Omega}} \tag{20b}$$

Finally, in the case of $\xi_L + \xi_T = 1$, R_f and μ are found from

$$\rho = \zeta\xi_L + \zeta\frac{1}{\sqrt{M\Omega}}\tan[\sqrt{M\Omega}(1 - \xi_L)] \tag{21a}$$

$$\mu = \frac{R_f}{-(\zeta M/2)\xi_L^2 + MR_f\xi_L + (1 - \zeta + \Omega)/\Omega} \tag{21b}$$

where R_f is the maximum value of ρ with respect to ξ_L.

Results. A plot of R_f versus M is shown in Figure 5 for values of Ω ranging from 0·0001 to ∞ and values of ζ equal to 0·75, 0·5 and 0·25. These curves were verified for Ω equal to ∞ using Murff[10] and with a numerical, finite difference model[13] for other values of Ω. For given values of Ω and ζ, the reduction factor decreases as M increases and ultimately approaches the limiting value of ζ. Hence, the available shear resistance along the interface decreases as M increases. M will increase as the interface stiffness increases ($M \propto \tau_p/\Delta_p$), as the axial stiffness of the waste decreases ($M \propto 1/EA$), and as the length of the slip surface increases ($M \propto L^2$). Note that M is plotted on a logarithmic scale in Figure 5.

At a given value of M, R_f decreases as Ω increases. The more sudden the post-peak reduction in resistance occurs with displacement, the greater the reduction in available shear resistance due to strain softening. The results in Figure 5 indicate that Ω has a substantial effect on the potential for progressive failure. For example, consider an Ω value of 1·0. Significant reductions in available

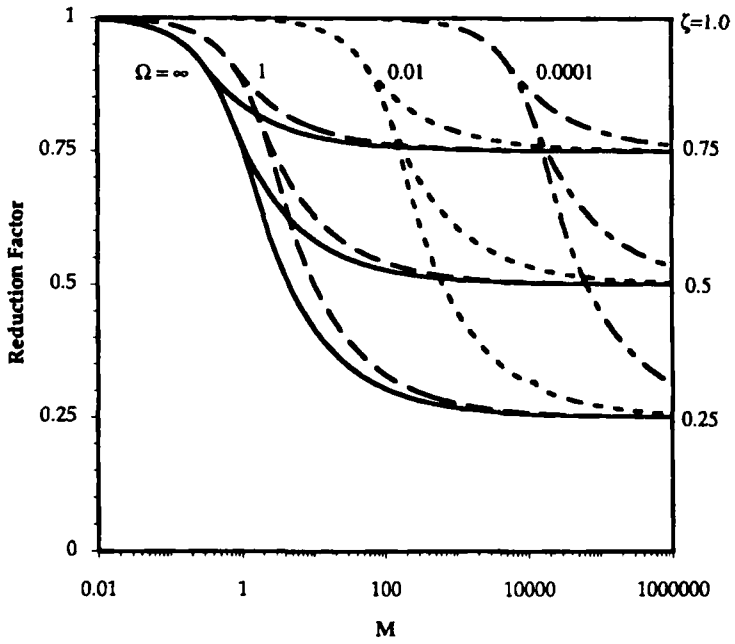

Figure 5. Average reduction in interface shear resistance versus non-dimensional factor M for compressible waste buttress — effect of strain-softening rate

shear strength occur for M values exceeding 1; however, this limiting M value increases to about 10,000 for an Ω value of 0·0001. In general, the limiting M value at which strain-softening effects become significant is insensitive to ζ and roughly approximated by $1/\Omega$ for $\Omega \leqslant 1$.

A plot of μ versus M is shown in Figure 6 for Ω values ranging from 0 to ∞ and ζ values ranging from 0·25 to 0·75. The solution is essentially insensitive to Ω and ζ. For M values less than about 1, the reduction in stiffness is negligible; however, the stiffness of the waste buttress decreases substantially as M increases for M values exceeding 1. The stiffness reduction factor μ can roughly be approximated by $1/M$ for $M \geqslant 1$ (Figure 6).

Slope case

Like the buttress, the slope is modelled as a compressible waste column on a strain-softening interface (Figure 3). However, a shear stress, $f(x)$, where x is the distance from the left boundary, is applied along the length of the slope to represent the driving force due to the weight of the waste. Since the depth of waste increases linearly along the slope length, $f(x)$ will be a linear function of x:

$$f(x) = f_S\left(\frac{x}{L_S}\right) \tag{22}$$

where L_S is the slope length and f_S is the applied shear stress at the toe of the slope. Further, the cross-sectional area of the waste column is also a linear function of x:

$$A_S(x) = H_S\left(\frac{x}{L_S}\right) W_1 \tag{23}$$

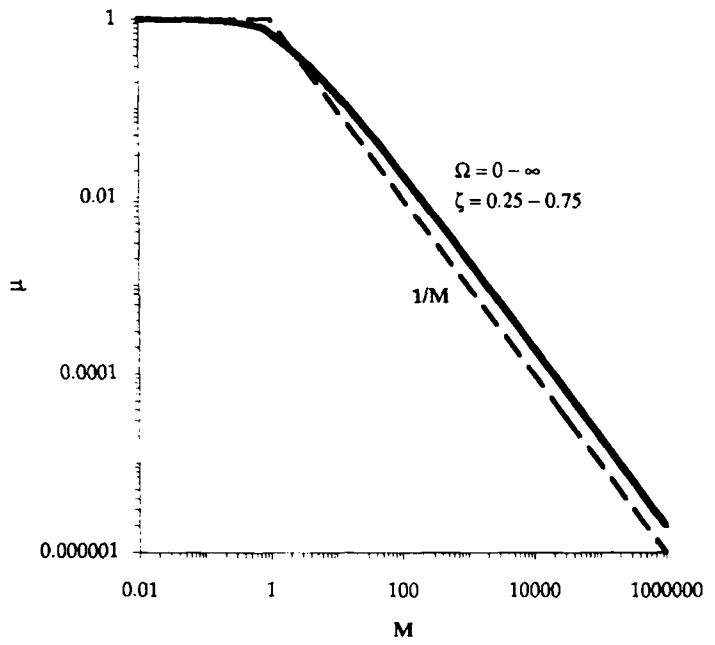

Figure 6. Buttress stiffness reduction factor μ versus non-dimensional factor M for compressible waste buttress

where $A_S(x)$ is the cross-sectional area as a function of x, and H_S is the height of the column at the toe of the slope and W_1 is the unit width of the column.

General solution. The relative displacement, u, along the interface is obtained from the following equation describing force equilibrium:

$$\frac{d}{dx}\left[A_S(x)\frac{du}{dx}\right] = \frac{[\tau(u,x) - f(x)]W_1}{E} \tag{24}$$

where $\tau(u,x)$ is the interface shear resistance and E is Young's modulus for the waste. If equations (22) and (23) are substituted into equation (24), then the following is obtained:

$$H_S\left(\frac{x}{L_S}\right)\frac{d^2u}{dx^2} + \left(\frac{H_S}{L_S}\right)\frac{du}{dx} = \frac{\tau(u,x) - f_S\left(\dfrac{x}{L_S}\right)}{E} \tag{25}$$

The following assumptions will be made to simplify the solution of this equation. First, we will assume that the peak and residual shear resistances, τ_p and τ_r, respectively (Figure 4), are directly proportional to normal stress. Second, we will assume that the peak and residual displacements, δ_p and δ_r, respectively (Figure 4), are independent of normal stress. These assumptions are consistent with the behaviour of common interfaces in containment systems. The interface shear resistance can now be expressed as a linear function of x:

$$\tau(u,x) = \tau_S(u)\left(\frac{x}{L_S}\right) \tag{26}$$

where $\tau_S(u)$ is the resistance at the toe of the slope for relative displacement u. If equation (26) is substituted into equation (25), the following equation is obtained:

$$\frac{d^2u}{dx^2} + \left(\frac{1}{x}\right)\frac{du}{dx} = \frac{[\tau_S(u) - f_S]}{EH_S} \tag{27}$$

To further simplify the problem, we will assume that the $(1/x)(du/dx)$ term in equation (27) can be neglected. This assumption is conservative because it effectively reduces the stiffness of the waste column; the resulting error will be explored later in this section. Equation (27) is therefore approximated by the following linear, partial differential equation with constant coefficients:

$$\frac{d^2u}{dx^2} = \frac{[\tau_S(u) - f_S]}{EH_S}. \tag{28}$$

Note that equation (28) describes force equilibrium for a column where the applied shear stress is uniform, the cross-sectional area is constant and the mobilized shear resistance is independent of normal stress.

Non-dimensional forms of equation (28) for the possible range of u values are given as follows:

$$\frac{d^2\upsilon}{d\xi^2} = M\upsilon - M\beta\Delta_p, \quad \upsilon \leqslant \Delta_p \tag{29a}$$

$$\frac{d^2\upsilon}{d\xi^2} = -M\Omega\upsilon + M(1 + \Omega - \beta)\Delta_p, \quad \Delta_p < \upsilon \leqslant \Delta_r \tag{29b}$$

$$\frac{d^2\upsilon}{d\xi^2} = (\zeta - \beta)M\Delta_p, \quad \upsilon > \Delta_r \tag{29c}$$

where $\upsilon = u/W_1$, $\Delta_p = \delta_p/W_1$, $\Delta_r = \delta_r/W_1$, $\xi = x/L_S$, $\beta = f_S/(\tau_p)_S$, and M is defined as

$$M = \frac{[(\tau_p)_S L_S]/\delta_p}{(EH_S)/L_S} \tag{30}$$

where L_S is the slope length, H_S is the column height at the toe of the slope and $(\tau_p)_S$ is the peak shear resistance evaluated at the toe. The general solution for equation (30) is given by

$$\upsilon = a_1 e^{\sqrt{M}\xi} + a_2 e^{-\sqrt{M}\xi} + \beta\Delta_p, \quad \upsilon \leqslant \Delta_p \tag{31a}$$

$$\upsilon = b_1 \cos(\sqrt{M\Omega}\xi) + b_2 \sin(\sqrt{M\Omega}\xi) + \left(\frac{1 + \Omega - \beta}{\Omega}\right)\Delta_p, \quad \Delta_p < \upsilon \leqslant \Delta_r \tag{31b}$$

$$\upsilon = \left[\frac{(\zeta - \beta)M\Delta_p}{2}\right]\xi^2 + c_1\xi + c_2, \quad \upsilon > \Delta_r \tag{31c}$$

where a_1, a_2, b_1, b_2, c_1 and c_2 are constants that depend on the boundary conditions.

Boundary conditions. The boundary conditions for the slope case are no external force applied to the left boundary (the slope crest) and a resistance at the right boundary (the slope toe) provided

by the buttress. Idealizing the buttress resistance by a linear spring with stiffness Q, the boundary conditions are expressed as

$$\left.\frac{d\upsilon}{d\xi}\right|_{\xi=0} = 0 \tag{32a}$$

$$\left.\frac{d\upsilon}{d\xi}\right|_{\xi=1} = -\alpha\upsilon|_{\xi=1} \tag{32b}$$

where

$$\alpha = \frac{QL_S}{EA_S} \tag{33}$$

and a negative force is compressive. Imposing these boundary conditions, we find the available shear resistance along the slope by comparing the buttress force mobilized at the toe with the applied shear force.

In the general case, the interface will be divided into a plastic zone near the crest where $\upsilon > \Delta_r$, a transition zone in the middle where $\Delta_p < \upsilon \leqslant \Delta_r$ and an elastic zone near the toe where $\upsilon \leqslant \Delta_p$. If the proportions of total length in the plastic and transition zones are denoted ξ_L and ξ_T, respectively, then the solution for υ is obtained from equation (31) by setting $\upsilon = \Delta_r$ at $\xi = \xi_L$ and $\upsilon = \Delta_p$ at $\xi = \xi_L + \xi_T$:

$$\frac{\upsilon}{\Delta_p} = \frac{(\zeta-\beta)M}{2}(\xi^2 - \xi_L^2) + \frac{1-\zeta+\Omega}{\Omega}, \quad 0 \leqslant \xi < \xi_L \tag{34a}$$

$$\frac{\upsilon}{\Delta_p} = \left(\frac{\beta-\zeta}{\Omega}\right)\cos[\sqrt{M\Omega}(\xi-\xi_L)] + \left[\frac{\beta-(\beta-\zeta)\cos(\sqrt{M\Omega}\xi_T)-1}{\Omega\sin(\sqrt{M\Omega}\xi_T)}\right] \times \sin[\sqrt{M\Omega}(\xi-\xi_L)] + \frac{1+\Omega-\beta}{\Omega}, \quad \xi_L \leqslant \xi < \xi_L + \xi_T \tag{34b}$$

$$\frac{\upsilon}{\Delta_p} = \frac{[(1-\beta)(1-\sqrt{M}/\alpha)e^{-\sqrt{M}} + \beta e^{-\sqrt{M}(\xi_L+\xi_T)}]e^{\sqrt{M}\xi}}{-(1+\sqrt{M}/\alpha)e^{\sqrt{M}(1-\xi_L-\xi_T)} + (1-\sqrt{M}/\alpha)e^{-\sqrt{M}(1-\xi_L-\xi_T)}} + \frac{-[(1-\beta)(1+\sqrt{M}/\alpha)e^{\sqrt{M}} + \beta e^{\sqrt{M}(\xi_L+\xi_T)}]e^{-\sqrt{M}\xi}}{-(1+\sqrt{M}/\alpha)e^{\sqrt{M}(1-\xi_L-\xi_T)} + (1-\sqrt{M}/\alpha)e^{-\sqrt{M}(1-\xi_L-\xi_T)}}, \quad \xi_L+\xi_T \leqslant \xi \leqslant 1 \tag{34c}$$

The values of ξ_L and ξ_T are evaluated by maintaining internal equilibrium at the boundary between the plastic and transition zones

$$\xi_L = \frac{1}{\sqrt{M\Omega}}\left[\frac{-(\beta-\zeta)\cos(\sqrt{M\Omega}\xi_T)+\beta-1}{(\zeta-\beta)\sin(\sqrt{M\Omega}\xi_T)}\right] \tag{35a}$$

and the boundary between the transition and elastic zones

$$\frac{(\beta-1)\cos(\sqrt{M\Omega}\xi_T)-\beta+\zeta}{\sqrt{\Omega}\sin(\sqrt{M\Omega}\xi_T)} = \frac{(1-\beta)[(1+\sqrt{M}/\alpha)e^{\sqrt{M}(1-\xi_L-\xi_T)} + (1-\sqrt{M}/\alpha)e^{-\sqrt{M}(1-\xi_L-\xi_T)}] + 2\beta}{-(1+\sqrt{M}/\alpha)e^{\sqrt{M}(1-\xi_L-\xi_T)} + (1-\sqrt{M}/\alpha)e^{-\sqrt{M}(1-\xi_L-\xi_T)}} \tag{35b}$$

The mobilized shear resistance, s_{mob}, is then found from force equilibrium as follows:

$$\frac{s_{mob}}{\tau_p} = \beta + \frac{1}{M}\left.\frac{d(\upsilon/\Delta_p)}{d\xi}\right|_{\xi=1} \tag{36}$$

where

$$\left.\frac{d(\upsilon/\Delta_p)}{d\xi}\right|_{\xi=1} = \frac{\sqrt{M}[2(1-\beta)+\beta(e^{\sqrt{M}(1-\xi_L+\xi_T)}+e^{-\sqrt{M}(1-\xi_L-\xi_T)})]}{-(1+\sqrt{M}/\alpha)e^{\sqrt{M}(1-\xi_L-\xi_T)}+(1-\sqrt{M}/\alpha)e^{-\sqrt{M}(1-\xi_L-\xi_T)}} \tag{37}$$

from equation (34). The derivative of υ with respect to ξ at the right boundary represents the compressive force carried by the buttress at the toe of the slope. This derivative is negative since the force is compressive; therefore, the mobilized shear resistance in equation (36) is the applied shear force less the buttress force.

The peak mobilized shear resistance is evaluated for the case of no strain softening, i.e. $\zeta = 1$. In this case, the mobilized shear resistance, s_{peak}, is given by

$$\frac{s_{peak}}{\tau_p} = \beta + \frac{1}{M}\left.\frac{d(\upsilon/\Delta_p)}{d\xi}\right|_{\xi=1} \tag{38}$$

where

$$\left.\frac{d(\upsilon/\Delta_p)}{d\xi}\right|_{\xi=1} = \frac{\sqrt{M}\{2\beta+(1-\beta)[(1+\sqrt{M}/\alpha)e^{\sqrt{M}(1-\xi_L)}+(1-\sqrt{M}/\alpha)e^{-\sqrt{M}(1-\xi_L)}]\}}{-(1+\sqrt{M}/\alpha)e^{\sqrt{M}(1-\xi_L)}+(1-\sqrt{M}/\alpha)e^{-\sqrt{M}(1-\xi_L)}} \tag{39}$$

and ξ_L is found from

$$\xi_L = \frac{2\beta+(1-\beta)[(1+\sqrt{M}/\alpha)e^{\sqrt{M}(1-\xi_L)}+(1-\sqrt{M}/\alpha)e^{-\sqrt{M}(1-\xi_L)}]}{(1-\beta)\sqrt{M}[-(1+\sqrt{M}/\alpha)e^{\sqrt{M}(1-\xi_L)}+(1-\sqrt{M}/\alpha)e^{-\sqrt{M}(1-\xi_L)}]} \tag{40}$$

The magnitude of the compressive force mobilized at the buttress for $\zeta = 1$ will be less than or equal to that mobilized for $\zeta < 1$; therefore, $s_{mob} \leq s_{peak}$. The average reduction in available shear resistance due to strain softening can be measured using a reduction factor given by

$$R_f = \frac{s_{mob}}{s_{peak}} \tag{41}$$

Note that s_{peak} is not necessarily equal to τ_p since the buttress may limit the relative displacements near the toe to less than those required to mobilize the peak shear resistance, δ_p (Figure 4). R_f will range from 1 (no reduction) to ζ (maximum reduction), and it is a function of the fundamental parameters M, ζ, Ω, α and β.

Similar to the buttress, the shear resistance may be mobilized before the plastic zone appears at the left boundary ($\xi_L = 0$) or after the elastic zone disappears from the right boundary ($\xi_L + \xi_T = 1$). In these cases, the solution for υ is obtained from equation (31) by modifying the boundary conditions accordingly. The derivative of υ/Δ_p with respect to ξ is then evaluated and substituted into equation (36) to find s_{mob} and, ultimately, R_f. For the case $\xi_L = 0$ and $\xi_T < 1$, the solution is given by

$$\left.\frac{d(\upsilon/\Delta_p)}{d\xi}\right|_{\xi=1} = \frac{\sqrt{M}\{2\beta+(1-\beta)[(1+\sqrt{M}/\alpha)e^{\sqrt{M}(1-\xi_T)}+(1-\sqrt{M}/\alpha)e^{-\sqrt{M}(1-\xi_T)}]\}}{-(1+\sqrt{M}/\alpha)e^{\sqrt{M}(1-\xi_T)}+(1-\sqrt{M}/\alpha)e^{-\sqrt{M}(1-\xi_T)}} \tag{42a}$$

where ξ_T is found from

$$\frac{\tan(\sqrt{M\Omega}\xi_T)}{\sqrt{\Omega}} = \frac{2\beta + (1-\beta)[(1+\sqrt{M}/\alpha)e^{\sqrt{M}(1-\xi_T)} + (1-\sqrt{M}/\alpha)e^{-\sqrt{M}(1-\xi_T)}]}{(1-\beta)[-(1+\sqrt{M}/\alpha)e^{\sqrt{M}(1-\xi_T)} + (1-\sqrt{M}/\alpha)e^{-\sqrt{M}(1-\xi_T)}]} \tag{42b}$$

When $\xi_L = 0$ and $\xi_S = 1$, the solution is expressed as

$$\left.\frac{d(v/\Delta_p)}{d\xi}\right|_{\xi=1} = \left(\frac{1+\Omega-\beta}{\cos(\sqrt{M\Omega}) - (\sqrt{M\Omega}/\alpha)\sin(\sqrt{M\Omega})}\right)\sqrt{\frac{M}{\Omega}}\sin(\sqrt{M\Omega}) \tag{43}$$

Finally, in the case of $\xi_L + \xi_T = 1$, the solution is given by

$$\left.\frac{d(v/\Delta_p)}{d\xi}\right|_{\xi=1} = \sqrt{\frac{M}{\Omega}}\left[(\zeta-\beta)\sin(\sqrt{M\Omega}\xi_T) - \frac{(\beta-\zeta)[\cos(\sqrt{M\Omega}\xi_T) - (\sqrt{M\Omega}/\alpha)\sin(\sqrt{M\Omega}\xi_T)] + 1 + \Omega - \beta}{(\beta-\zeta)[\sin(\sqrt{M\Omega}\xi_T) + (\sqrt{M\Omega}/\alpha)\cos(\sqrt{M\Omega}\xi_T)]}\right] \tag{44}$$

where ξ_T is found from

$$1 - \xi_T = \frac{1}{\sqrt{M\Omega}}\left(\frac{(\beta-\zeta)[\cos(\sqrt{M\Omega}\xi_T) - (\sqrt{M\Omega}/\alpha)\sin(\sqrt{M\Omega}\xi_T)] + 1 + \Omega - \beta}{(\beta-\zeta)[\sin(\sqrt{M\Omega}\xi_T) + (\sqrt{M\Omega}/\alpha)\cos(\sqrt{M\Omega}\xi_T)]}\right) \tag{45}$$

Results. A plot of R_f versus M is shown in Figure 7 for β equal to 2·5, α equal to 1·0, Ω values ranging from 0·0001 to ∞, and ζ values of 0·25, 0·5 and 0·75. These curves were verified with a numerical, finite difference model.[13] For any given value of Ω, the available shear resistance decreases as M increases. Similar to the buttress case (Figure 5), the reduction in shear resistance from peak to residual occurs rapidly with increasing M once a limiting value of M is exceeded. However, the rate of reduction is greater in the case of the slope because the driving load is applied as a shear stress distributed over the length of the slope; hence, the limiting M values for a given Ω value are smaller. Consider an Ω value of 0·0001. The reduction in available shear resistance occurs at an approximate M value of 10,000 for the buttress case (Figure 5), while it occurs at an approximate M value of 100 for the slope case (Figure 7). Therefore, it is more likely that the peak shear resistance of a given interface will be available along the base of the containment system versus the side slope.

A plot of R_f versus M is shown in Figure 8 for β values of 1·5, 2·5 and 3·5, Ω equal to 0·01, α equal to 1·0 and ζ values of 0·25, 0·5 and 0·75. As the applied shear stress increases (β increases), the reduction in shear resistance occurs at smaller values of M. However, the results in Figure 8 indicate that β does not affect the available shear resistance significantly. Note that strain softening will not occur in this model if β is less than or equal to 1·0.

A plot of R_f versus M is shown in Fig. 9 for α values ranging from 0·1 to ∞, Ω equal to 0·01, β equal to 2·5 and ζ values of 0·25, 0·5 and 0·75. As the spring stiffness increases, the reduction in available shear resistance due to strain softening occurs at greater M values. However, these effects are not significant for α values ranging from 1·0 to ∞. If μ in equation (17) is approximated by $1/M$ (Figure 6), then α can be approximated by

$$\alpha \approx \left(\frac{H_B}{L_B}\right)\left(\frac{L_S}{H_S}\right)\cos^2\theta \tag{46}$$

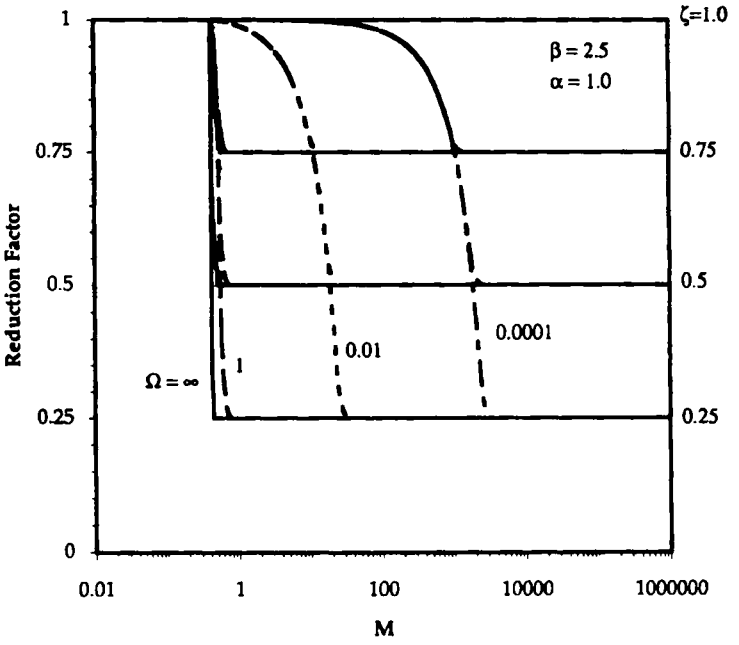

Figure 7. Average reduction in interface shear resistance versus non-dimensional factor M for compressible waste slope — effect of strain-softening rate

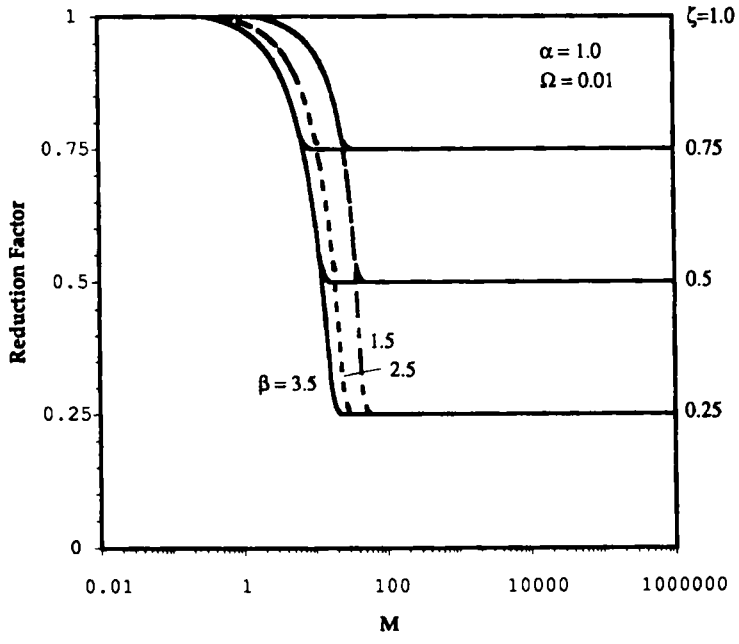

Figure 8. Average reduction in interface shear resistance versus non-dimensional factor M for compressible waste slope — effect of applied shear stress

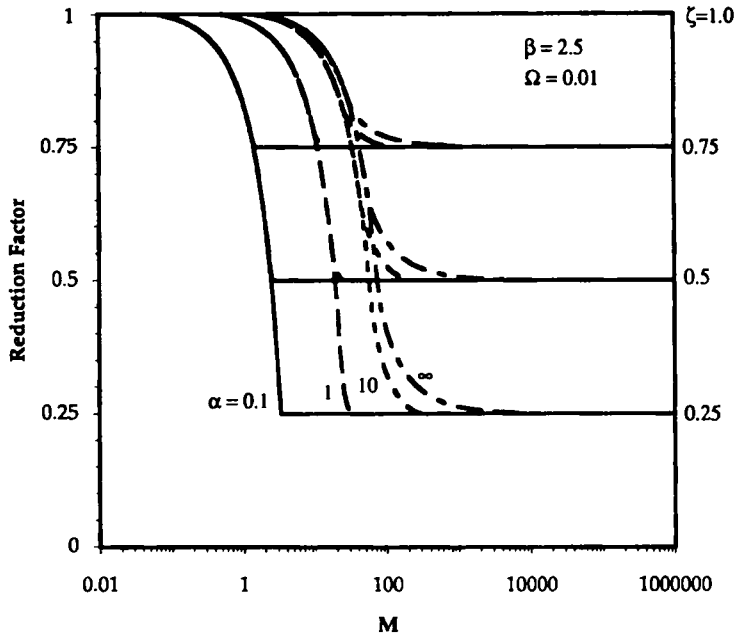

Figure 9. Average reduction in interface shear resistance versus non-dimensional factor M for compressible waste slope — effect of buttress stiffness

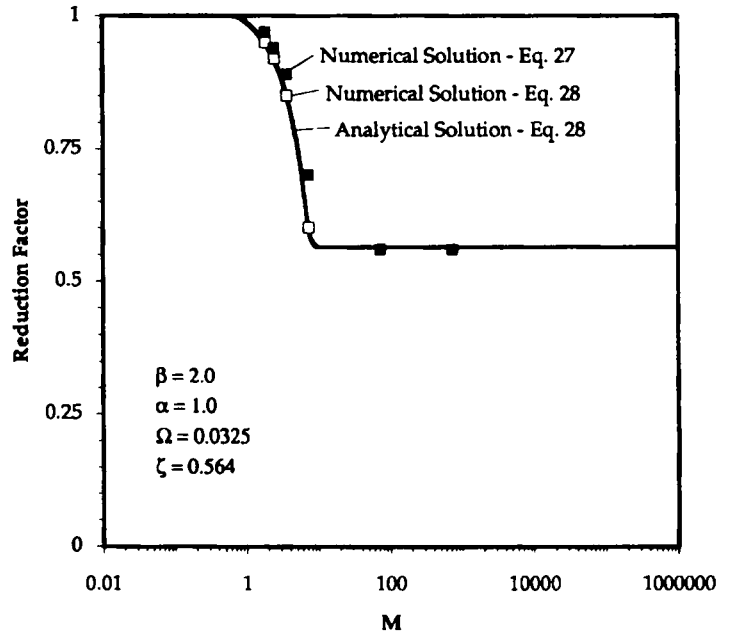

Figure 10. Comparison of analytical approximation with exact, numerical solution for compressible waste slope

where θ is the angle from horizontal at which the resultant force acts between the slope and buttress. For typical geometries, α will be less than or equal to 1·0. In summary, the most important parameters affecting the available shear resistance along the slope are M and Ω.

In developing these solutions, the partial differential equation describing force equilibrium was simplified, i.e. equation (27) was approximated by equation (28). A comparison of the approximate, analytical solution (equation (28)) with an exact, numerical solution of equation (27) is shown in Figure 10. The analytical solution is slightly conservative because the column stiffness is effectively reduced through the approximation; however, the approximate results are reasonably close to the exact solution for practical purposes.

CASE STUDY OF MODEL VALIDITY

The Kettleman Hills Phase 1A Landfill in California provides a valuable case study to investigate the validity of these non-dimensional solutions. A large slope failure occurred within this waste containment system in 1988 (References 1, 14, 15). The hazardous waste landfill cell was situated in a valley with an open end. A representative, two-dimensional cross-section of the slope that failed is shown in Figure 11. Approximately 450,000 m^3 of waste slid 10 m horizontally along the containment system. Post-failure investigations[1] indicated that the failure surface was located primarily at the interface between a geomembrane and a compacted clay liner (CM/Clay interface) on the landfill base, and at the interface between a geotextile and a geomembrane (GT/GM interface) on the side slope. Shear resistance versus displacement relationships for these interfaces (Figure 12) were derived from large-scale direct shear and torsional ring shear test results.[2] The waste was similar to a sand in composition with a unit weight of 17·2 kN/m^3, an angle of internal friction of 40°, and an assumed Young's modulus value of 7200 kPa (Reference 8).

One-dimensional analysis

The waste buttress is modelled as a column that is 27·5 m high (H_B) by 111 m long (L_B) (Figure 11). The normal stress along the interface at the column base due to is weight is 475 kPa, giving a peak shear resistance of 43·2 kPa (τ_p) and a residual shear resistance of 28·2 kPa (τ_r). The resulting non-dimensional parameters for the buttress are summarized in Table I (base case). Similarly, the side slope is 61·5 m long (L_S) and the waste thickness at the toe (H_S) is 30·7 m (Figure 11). At the toe of the slope, the normal stress on the interface due to the weight of waste is

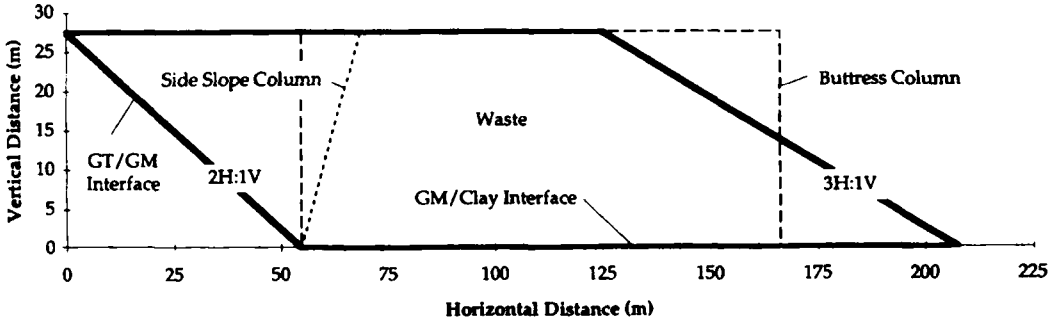

Figure 11. Representative, two-dimensional cross-section through Kettleman Hills landfill slope

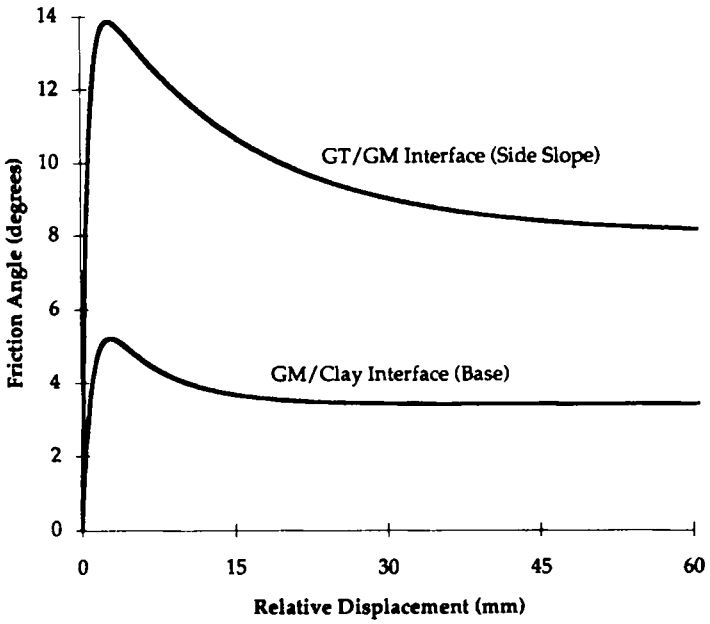

Figure 12. Shear stress versus displacement for critical interfaces in Kettleman Hills landfill slope

424 kPa while the applied shear stress is 212 kPa. The peak shear resistance at the toe is 106 kPa $[(\tau_p)_S]$ and the residual shear resistance is 59·6 kPa $[(\tau_r)_S]$. We will assume that the resultant force between the slope and the buttress (θ) acts at an angle of 40° (the internal friction angle of the waste) to the horizontal. The non-dimensional parameters for the side slope are also summarized in Table I (base case).

The curves in Figure 5 indicate that the available shear resistance on the landfill base is 67 percent of the peak resistance ($R_f = 0{\cdot}67$), while the curves in Figure 7–9 indicate that $R_f = 0{\cdot}56$ on the side slope (the residual strength is mobilized along the entire slope). If these estimated shear resistances are applied to the base and side slope in a limit equilibrium analysis and the orientation of the force between the base and side slope is assumed to be θ (40°), then the calculated factor of safety for this slope is 1·03. Since failure occurred at a slope height of about 27·5 m, the results from this simplified analysis are consistent with the observed failure of this slope.

Two-dimensional, numerical analysis

In order to explore the validity of simplifying this two-dimensional cross-section into two one-dimensional columns, a numerical analysis was performed to model the slope in two dimensions. The Universal Distinct Element Code (UDEC) developed by ITASCA[16] was used in this analysis. UDEC is a two-dimensional, numerical program based on the distinct element method. The waste was modelled as an elastic material with $\phi = 40°$, $c = 48$ *kPa*, $E = 7200$ kPa and $\nu = 0{\cdot}3$, while the interface shear resistances were modelled using the curves shown in Figure 11. The waste was discretized into 612 quadrilateral elements with 28 contact points along the interfaces. The waste height was increased in 0.15 m intervals until the mass became unstable.

Table I. Comparison of analytical and two-dimensional, numerical results for Kettleman Hills landfill slope

	One-dimensional analysis				Two-dimensional analysis		
	Non-dimensional parameters		Reduction factor		Reduction factor		
Case	Buttress	Slope	Buttress	Slope	Buttress	Slope	Height at failure (m)
Base case	$M = 1100$ $\zeta = 0{\cdot}65$ $\Omega = 0{\cdot}064$	$M = 720$ $\zeta = 0{\cdot}56$ $\Omega = 0{\cdot}033$ $\beta = 2{\cdot}0$ $\alpha = 0{\cdot}3$	0·67	0·56	0·68	0·56	28·1
Case 1	$M = 1100$ $\zeta = 0{\cdot}65$ **$\Omega = 0{\cdot}013$**	$M = 720$ $\zeta = 0{\cdot}56$ $\Omega = 0{\cdot}033$ $\beta = 2{\cdot}0$ $\alpha = 0{\cdot}3$	0·70	0·56	0·70	0·56	28·5
Case 2	**$M = 110$** $\zeta = 0{\cdot}65$ $\Omega = 0{\cdot}064$	**$M = 72$** $\zeta = 0{\cdot}56$ $\Omega = 0{\cdot}033$ $\beta = 2{\cdot}0$ $\alpha = 0{\cdot}3$	0·73	0·56	0·73	0·56	29·3
Case 3	**$M = 110$** $\zeta = 0{\cdot}65$ **$\Omega = 0{\cdot}013$**	**$M = 72$** $\zeta = 0{\cdot}56$ $\Omega = 0{\cdot}033$ $\beta = 2{\cdot}0$ $\alpha = 0{\cdot}3$	0·82	0·56	0·83	0·56	32·0

A maximum, stable waste height of 28·1 m was obtained in this analysis, which is consistent with the observed failure at a waste height of about 27·5 m and with the results from the one-dimensional analysis. The mobilized shear resistances at this maximum waste height were integrated along each interface, and the average resistance along the base was 68 percent of the peak while that along the side slope was 56 percent of the peak. These results are comparable to those obtained from the simplified, one-dimensional analysis (base case in Table I).

Parametric study

A parametric study of the Kettleman Hills landfill slope was conducted to compare results further from the one- and two-dimensional analyses. First, the rate of strain softening at the buttress interface was reduced by a factor of about five (Case 1 in Table I). This strain-softening rate is comparable to that for the GT/GM interface. Second, the waste stiffness, E, was increased by an order of magnitude (Case 2 in Table I). This modulus represents an upper limit on the range of modulus values for typical hazardous waste materials.[17] Finally, both the strain-softening rate for the interface and the modulus value for the waste were varied (Case 3 in Table I). In all cases, results from the one-dimensional analysis compare favourably with those from the two-dimensional analysis. Note that the available shear resistance along the side slope is equal to the residual resistance, even for Case 3. The curves in Figs 7–9 indicate that more than a two-order of magnitude increase in the waste modulus would be required before the available shear resistance on the side slope is greater than the residual.

Limitations of results

While results from the one- and two-dimensional analyses compare favourably to each other and to the observed field behaviour in one case, it is important to point out the limitations associated with both analyses. First, waste materials are not elastic. In the two-dimensional analysis, some yielding occurred within the waste prior to failure of the slope. The resulting stress redistribution reduced deformations at the interface; hence, it was conservative to assume the waste to be elastic for this geometry. Second, waste fills are three-dimensional, not two-dimensional structures. Finally, deformations will occur as waste is placed in the landfill. Therefore, while these results are useful and promising, they should be used with caution.

CONCLUSIONS

An analytical approach to evaluate strain-softening effects on the stability of waste containment systems is presented. The shear resistance provided by the containment system is modelled using an idealized piecewise linear function that incorporates a finite rate of strain softening with displacement. The waste is modelled using one-dimensional, elastic columns. Results are presented in a non-dimensional form to relate strain-softening effects to the properties of the waste, the properties of the containment system interface and the geometry of the slope. The potential for progressive failure increases as (i) the waste stiffness decreases relative to the initial stiffness of the interface, (ii) the length of the slip surface increases and (iii) the rate of strain softening with displacement increases. In addition, strain-softening behaviour is more likely to reduce the available shear resistance along a side slope than along the base of a containment system. Analysis of a case study slope failure indicates that the analytical approach produces results that are consistent with field observations and comparable to results from a two-dimensional, numerical analysis. Although simple, this analytical approach serves as a useful design guide to identify cases where it is unsafe to use the peak shear strength in a limit equilibrium analysis.

APPENDIX I

Notation

A	cross-sectional area of column
a	constant of integration
b	constant of integration
c	constant of integration
E	Young's modulus of column
f	shear stress applied to column
H	height f column
L	length of column
M	$[(\tau_p L)/\delta_p]/[(EH)/L]$
P	force applied to column
Q	spring stiffness
R_f	average reduction in available shear resistance due to strain softening
s	average shear resistance
u	relative displacement at interface
W	width of column

x	distance along column
α	QL/EA
β	f/τ
Δ	δ/W
δ	relative shear displacement required to mobilize shear resistance τ
ζ	τ_r/τ_p
θ	angle of inclination from horizontal at which resultant force acts between slope and buttress
μ	Q_{max}/Q_{peak}
ν	u/W and Poisson's ratio
ξ	x/L
ρ	average reduction in mobilized shear resistance due to strain softening
τ	shear resistance
Φ	$[(P/W)/EA]L$
ϕ	angle of internal friction
Ω	$[-(\tau_r - \tau_p)/(\delta_r - \delta_p)]/(\tau_p/\delta_p)$

Subscripts

B	buttress
L	plastic zone
max	maximum
mob	mobilized
p	peak
r	residual
S	slope
T	transition zone
1	unit

REFERENCES

1. R. J. Byrne, J. Kendall and S. Brown, 'Cause and mechanism of failure, Kettleman Hills Landfill B-19, Unit IA', *Proc., ASCE Sopec. Conf. on Performance and Stability of Slopes and Embankments — II*, Vol. 2, 1992, pp. 1188–1215.
2. T. D. Stark and A. R. Poeppel, 'Landfill linear interface strengths from torsional ring shear tests', *J. geotech. eng. div. ASCE*, **120**(3), 597–615 (1994).
3. S. Bernander and I. Olofsson, 'On formation of progressive failures in slopes', *Proc. 10th ICSMFE*, Stockholm, 1981, pp. 357–362.
4. N.-E. Wiberg, M. Koponen and K. Runesson, 'Finite element analysis of progressive failure in long sloes', *Int. j. numer. anal. methods geomech.*, **14**, 599–612 (1990).
5. J.M. Duncan and P. Dunlop, 'Slopes in stiff-fissured clays and shales', *J. Geotech. eng. div. ASCE* **95**(2), 467–492 (1969).
6. K.Y. Lo and C.F. Lee, 'Stress analysis and slope stability in strain-softening materials', *Geotechnique*, **23**(1), 1–11 (1973).
7. K.T. Law and P. Lumb, 'A limit equilibrium analysis of progressive failure in the stability of slopes', *Can. Geotech. J.*, **15**, 113–122 (1978).
8. R. J. Byrne, 'Design issues with strain-softening interfaces in landfill liners', *Proc. Waste Tech '94*, Charleston, SC, 1994.
9. J. T. Christian and R. Whitman, 'One-dimensional model for progressive failure', *Proc. 7th ICSMFE*, Mexico City, 1969, pp. 541–545.
10. J. D. Murff, 'Pile capacity in a softening soil', *Int. j. Numer. Anal. Methods Geomech.*, **4**(2), 185–189 (1980).
11. M.F. Randolph, 'Design considerations for offshore piles', *Proc. Conf. on Geotech. Practice in Offshore Eng.*, ASCE, Austin, TX, 1983, pp. 422–439.

12. K. Y. Lo, 'An approach to the problem of progressive failure', *Can. Geotech. J.*, **9**(4), 407–429 (1972).
13. R. B. Gilbert, J. H. Long and J. J. Daly, 'Structural integrity of compositegeosynthetic lining and cover systems', *Proc., Geosynthetics '93*, Vancouver, BC, 1993, pp. 1389–1403.
14. J. K. Mitchell, R. B. Seed and H. B. Seed, 'Kettleman Hills waste landfil slope failure. I: Liner system properties', *J. geotech eng. duiv. ASCE*, **116**(4), 647–668 (1990).
15. R. B. Seed, J. K. Mitchell and H. B. Seed, 'Kettleman Hills waste landfill slope failure. II: Stability analyses', *J. geotech. eng. div. ASCE*, **116**(4), 669–690 (1990).
16. ITASCA, 'UDEC, Universal Distinct Element Code, Version 2.0, Volume I: User's Manual', ITASCA Consulting Group, Minneapolis, MN, 1993.
17. I. S. Oweis and R. P. Khera, *Geotechnology of Waste Management*, Butterworths, London, 1990.